Image-Based Spatial Shading Analysis for Power Performance Degradation in Photovoltaic Systems

[1]Andi Makkulau, [2] Ramlah, [3]Alex Fernandes, [4]Syaripudin Ardiansyah
[1,3,4] Faculty of Electricity and Renewable Energy, Institut Teknologi PLN, Jakarta Indonesia
[2] Faculty of Infrastructure and Regional Technology, Institut Teknologi PLN, Jakarta Indonesia
[1] andi.mk@itpln.ac.id, [2]ramlah@itpln.ac.id, [3]alex.fernandes@itpln.ac.id, [4]syaripudin.a@itpln.ac.id

Abstract - ***Partial shading is one of the dominant causes of energy performance degradation in static photovoltaic (PV) systems, especially in tropical environments where dust accumulation and vegetation growth frequently occur. Conventional shading analysis in photovoltaic energy studies is commonly conducted using geometric simulation or irradiance-based modelling without explicitly identifying physical shading objects on the PV surface. This paper proposes a computer vision-based approach to quantitatively detect shading objects and statistically evaluate their impact on PV energy performance. A Python–OpenCV framework was developed to calculate pixel-based shading area on a 10 Wp static PV module. Electrical parameters including voltage, current, and output power were experimentally measured under shading levels ranging from 10% to 100%. Statistical analyses consisting of Pearson correlation, linear regression, significance testing, and one-way Analysis of Variance (ANOVA) were applied. The results show a very strong negative correlation between shading area and both current and power output ($r = -0.98$, $p < 0.001$). Linear regression indicates that shading area explains 96.1% of current variation ($R^2 = 0.961$), while ANOVA confirms statistically significant differences in energy output across shading levels ($p < 0.01$). These findings demonstrate that computer vision-based shading quantification provides a statistically robust and energy-oriented framework for analysing performance degradation in static photovoltaic systems.***

Keywords — Photovoltaic Energy, Partial Shading, Computer Vision, Energy Loss, Statistical Analysis

I. Introduction

Photovoltaic (PV) systems have become one of the fastest-growing renewable energy technologies due to their scalability, low maintenance requirements, and decreasing installation costs, making them an important component of sustainable electricity generation [1], [2]. However, the electrical performance of PV systems is highly dependent on operating conditions, and their actual power output often deviates from the rated capacity because of environmental factors such as temperature variations, dust accumulation, cloud cover, module aging, and partial shading. Among these factors, partial shading is particularly critical because it not only reduces the incident solar irradiance but also introduces electrical mismatch in series-connected PV cells, leading to significant output power degradation. Therefore, accurate identification and quantification of shading effects are essential for improving photovoltaic performance evaluation and maintenance strategies. Among various renewable energy technologies, photovoltaic (PV) systems have gained significant attention because of their modularity, scalability, low maintenance requirements, and continuously declining installation costs [3], [4]. Over the past decade, substantial improvements in PV conversion efficiency, manufacturing processes, and power electronics have further enhanced the economic viability of solar energy systems. Countries located in tropical regions, including Indonesia, possess substantial solar energy potential due to their relatively stable solar irradiance throughout the year [5]. Consequently, photovoltaic deployment has become an attractive strategy for increasing renewable energy penetration while improving energy security and reducing dependence on conventional fossil-fuel-based power generation. Nevertheless, the actual performance of PV installations frequently differs from expected theoretical outputs because PV systems operate under dynamic environmental conditions that are difficult to predict accurately [6], [7]. Factors such as temperature variation, dust accumulation, cloud cover, module aging, and shading conditions significantly influence system efficiency and energy yield. Therefore, understanding and mitigating performance degradation mechanisms remains essential for maximizing the effectiveness and reliability of photovoltaic energy systems.

Among the various environmental disturbances affecting photovoltaic systems, partial shading is widely recognized as one of the most significant factors contributing to energy loss and efficiency reduction [8], [9]. Partial shading occurs when only a portion of the PV module surface receives reduced solar irradiance due to obstructions such as nearby buildings, vegetation, utility poles, accumulated debris, or temporary objects that block sunlight reaching the module surface [10]. Unlike uniform irradiance reduction, partial shading creates electrical mismatch conditions among interconnected solar cells because PV modules are typically composed of series-connected cells [11]. Under such circumstances, shaded cells limit the current flow of the entire string, resulting in disproportionate reductions in output power relative to the shaded area [12]. Furthermore, severe shading conditions may trigger reverse bias operation in affected cells, leading to hotspot formation and accelerated material degradation that can shorten module lifespan [8], [13]. These technical consequences not only reduce energy production but also increase operational and maintenance costs over the long term. As photovoltaic installations continue to expand in urban, residential, and industrial environments where shading sources are unavoidable, accurate assessment of shading impacts has become increasingly important. Consequently, reliable methods for quantifying shading-induced energy losses are necessary to support performance monitoring, maintenance planning, and optimization of photovoltaic system operation.

To evaluate the influence of shading on photovoltaic performance, numerous researchers have developed simulation-based approaches that estimate energy losses using geometric and electrical models. Software platforms such as PVsyst, System Advisor Model (SAM), and Helioscope have become widely adopted tools for predicting photovoltaic energy yield under various environmental and operational conditions [14], [15]. These tools integrate solar irradiation data, module specifications, array configurations, and shading geometries to estimate annual energy production and performance ratios [16]. Their application has proven highly beneficial during the planning and design stages of photovoltaic projects because they enable engineers to assess alternative system configurations and optimize installation layouts before deployment [17]. However, despite their effectiveness, these simulation platforms generally rely on predefined shading assumptions and simplified geometric representations of shading objects, where the size, shape, position, and orientation of obstructions are specified manually based on idealized models rather than actual field observations [18]. Consequently, complex and irregular shading patterns caused by vegetation, surrounding buildings, utility poles, or other real-world obstacles are often difficult to represent accurately, potentially leading to discrepancies between simulated and actual photovoltaic performance. In many practical situations, shading conditions are highly dynamic and involve irregularly shaped obstructions whose characteristics are difficult to represent accurately within conventional simulation environments [19]. Consequently, discrepancies may arise between simulated energy loss estimates and actual field conditions. Moreover, most simulation-based studies focus on long-term energy yield assessment rather than direct quantification of physical shading observed on module surfaces. These limitations highlight the need for complementary approaches capable of capturing real-world shading conditions and translating them into meaningful indicators of photovoltaic performance degradation.

Experimental investigations have also been conducted to understand the electrical behaviour of photovoltaic modules subjected to partial shading conditions. Previous studies commonly analyze the variations in voltage, current, power output, fill factor, and efficiency under controlled shading scenarios [20], [21]. Their findings consistently indicate that current is significantly more sensitive to shading than voltage because current generation in series-connected photovoltaic cells depends directly on the least illuminated section of the module [22]. As a result, even relatively small shaded areas may cause substantial reductions in power output, revealing the nonlinear relationship between shading coverage and electrical performance degradation [23]. Although these studies have contributed valuable insights into photovoltaic behaviour under shading conditions, most experiments rely on predefined shading patterns generated using artificial obstacles with known dimensions [24], [25]. While such approaches facilitate controlled laboratory investigations, they do not adequately represent the complexity of shading conditions encountered in actual photovoltaic installations. In real operating environments, shading patterns frequently exhibit irregular shapes, varying intensities, and continuously changing positions due to environmental dynamics. Consequently, existing experimental methods often lack a quantitative mechanism for accurately measuring the actual shaded area and correlating it directly with electrical energy losses. This limitation creates uncertainty in evaluating the true impact of shading on photovoltaic system performance. To address this limitation, an image-based spatial shading analysis approach is proposed in this study. By combining computer vision techniques with pixel-based shading area quantification and statistical analysis of photovoltaic electrical parameters, the proposed method enables direct measurement of physical shading coverage and its relationship with output power degradation under controlled experimental conditions.

Recent developments in computer vision, digital image processing, and artificial intelligence have opened new opportunities for non-contact monitoring and assessment of energy systems. Advances in imaging technologies, computational power, and machine learning algorithms have enabled automatic extraction of useful information from visual data across various engineering applications [26], [27]. Within the photovoltaic sector, image-based techniques have been widely employed for defect detection, crack identification, dust accumulation monitoring, and thermal anomaly analysis using RGB, multispectral, and infrared imagery [28], [29]. These approaches provide rapid, cost-effective, and scalable alternatives to conventional inspection methods, particularly for large-scale solar installations [30]. Furthermore, image processing techniques enable detailed characterization of module surface conditions without interrupting normal system operation [31].Specifically, previous studies have demonstrated that computer vision methods are effective for identifying surface defects, detecting cracks, monitoring soiling conditions, and recognizing thermal anomalies with high accuracy. However, these studies primarily utilize image analysis as a diagnostic or classification tool, where the outputs are limited to identifying the presence, location, or type of anomaly rather than quantifying its electrical consequences [28]–[31]. Other studies have incorporated artificial intelligence algorithms to improve the automation and reliability of photovoltaic inspection, yet their performance evaluation remains focused on detection accuracy instead of establishing quantitative relationships between visual features and electrical output parameters [32], [33]. Despite the growing adoption of vision-based monitoring approaches, the majority of existing studies focus primarily on classification, fault detection, or condition assessment tasks rather than direct energy performance evaluation [32]. Most image-based methods are designed to identify the presence or location of defects and shading without quantitatively measuring the actual shading area on the photovoltaic surface. Furthermore, pixel-based shading measurements are rarely integrated with statistical analyses to establish quantitative relationships between image-derived shading coverage and electrical output parameters such as voltage, current, and output power.

Recent advances in computer vision have enabled more efficient and accurate photovoltaic monitoring; however, most existing studies remain focused on defect detection, anomaly classification, and condition assessment rather than quantitative energy performance evaluation. Although these approaches are effective for identifying the presence and location of shading or faults, limited attention has been devoted to transforming image-derived shading information into quantitative variables that can be directly linked to photovoltaic electrical performance. Consequently, the potential of computer vision for estimating shading-induced energy degradation remains insufficiently explored.

Despite significant advancements in photovoltaic monitoring and shading analysis, a substantial research gap remains regarding the integration of visual shading information with quantitative energy loss estimation. Existing simulation studies provide valuable predictive capabilities but often depend on simplified assumptions that may not accurately reflect real operating conditions. Similarly, experimental investigations demonstrate the effects of shading on electrical output but rarely incorporate detailed measurements of actual shaded surface areas. Meanwhile, computer vision applications in photovoltaics predominantly focus on detection and classification tasks without explicitly translating visual shading characteristics into electrical performance metrics [33]. Consequently, the relationship between image-detected shading coverage and photovoltaic energy losses remains insufficiently understood [34]. Addressing this gap is important because practical maintenance decisions require not only identifying shading objects but also understanding their impact on system energy production. Therefore, this study proposes an image-based spatial shading analysis approach for evaluating electrical energy losses in photovoltaic systems. The novelty of this research lies in the integration of computer vision techniques with photovoltaic performance analysis to quantitatively determine shaded surface areas and investigate their correlation with electrical parameters such as voltage, current, and power output. The findings are expected to contribute to the development of intelligent photovoltaic monitoring systems capable of providing more accurate, data-driven assessments of shading-induced energy losses and supporting more effective operation and maintenance strategies for solar energy installations.

II. Research Method

A. Experimental Setup

The experimental system consisted of a static photovoltaic (PV) module with a nominal capacity of 10 Wp. The module was operated under laboratory-scale conditions to minimize uncontrolled environmental variations. The photovoltaic module was illuminated using natural sunlight during clear-sky conditions, while all experiments were conducted within a limited time window to minimize fluctuations in solar irradiance and illumination intensity. This approach ensured consistent image acquisition conditions and reduced variations in HSV values caused by changes in ambient lighting. A digital camera was positioned perpendicular to the PV surface to capture images of shading conditions. The camera used in this study was a *web cam* with an image resolution of *720* pixels and a focal length of *35* mm. The camera was mounted at a fixed distance of *20* cm from the PV module, with its optical axis aligned perpendicular (90°) to the module surface to minimize perspective distortion. All images were acquired using the same camera settings and geometric configuration throughout the experiment to ensure consistent image quality and reliable shading area quantification. The electrical output parameters, namely DC voltage and current, were measured using a calibrated digital multimeter. Shading objects were systematically applied to the PV surface to produce controlled shading levels ranging from 10% to 100%.

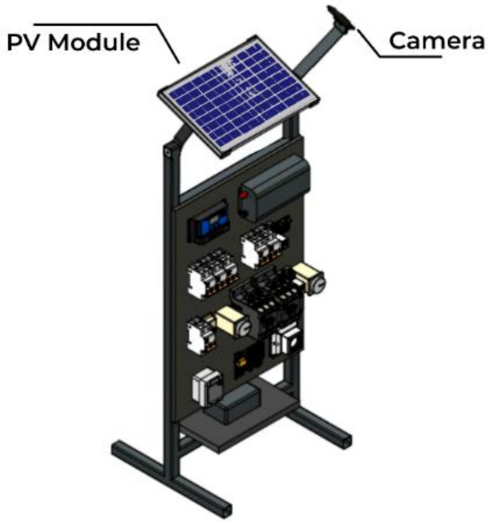

Figure 1 Experimental system setup

B. Computer Vision-Based Shading Quantification

An image-based, computer vision–assisted approach is employed to spatially quantify shading distribution on the photovoltaic module surface. The computer vision approach was employed to transform physical shading objects into a quantitative parameter. Captured RGB images were converted into the HSV color space to improve robustness against illumination variations. Object segmentation was performed using binary masking. The segmentation process employed fixed HSV threshold values of HSVmin = (Hmin, Smin, Vmin) and HSVmax = (Hmax, Smax, Vmax), where pixels with HSV values within this range were classified as shading objects, while all remaining pixels were assigned to the background.

These threshold values were determined through preliminary experimental calibration to ensure accurate separation between the shading object and the photovoltaic module surface under the controlled lighting conditions used in this study.
Object segmentation was performed using binary masking:

$$M(x,y) = \begin{cases} 1, & HSV_{min} \leq HSV\ (x,y) \leq HSV_{max} \\ 0, & otherwise \end{cases} \quad (1)$$

where $M_{(x,y)}$ represents the binary mask at pixel coordinate (x,y) and HSV_{min} and HSV_{max} define the color thresholds corresponding to shading objects.
The shading area percentage was calculated using a pixel-based method:

$$A_s\ (\%) = \frac{N_{object}}{N_{total}}\ x\ 100\% \quad (2)$$

Where:
A_s : Percentage of shading (%)
N_{object} : number of white pixels (object)
N_{total} : total of PV surface pixels

where N_{object} represents the number of pixels corresponding to shading objects and N_{total} represents the total number of pixels covering the PV surface. To generate repeatable shading conditions, a flat, matte black rectangular plate was used as the shading object throughout all experiments. The matte surface minimized specular reflections, while the rectangular geometry provided well-defined and reproducible shading patterns on the PV module. The object was positioned at predetermined locations to produce different shading coverage levels. Its high visual contrast relative to the PV surface facilitated consistent segmentation using the predefined HSV threshold values, enabling accurate quantification of the shaded area and subsequent correlation with the measured output power degradation.

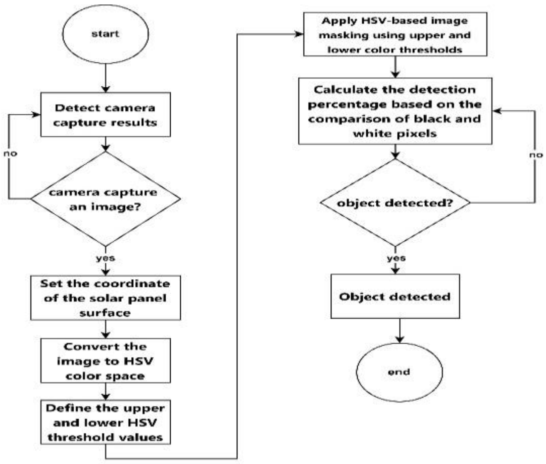

Figure 2 The computer vision workflow.

Figure 2 Computer vision workflow illustrating image acquisition, pre-processing, color space conversion, object segmentation, and pixel-based shading area quantification used as input for photovoltaic energy performance analysis.

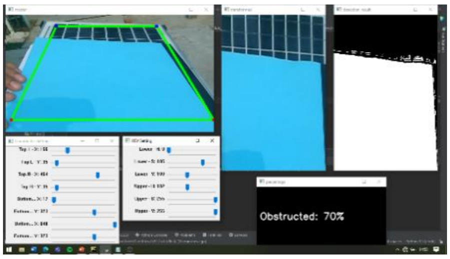

Figure 3 visual result image-based shading detection

Figure 3 presents the visual results of the image-based shading detection applied to the photovoltaic module surface. The detected shading objects are spatially segmented using colour-based thresholding, allowing clear differentiation between shaded and unshaded regions. The shaded areas are highlighted in binary form, where the detected object regions are represented in white, while the unshaded photovoltaic surface is represented in black. This visualization confirms that the proposed image-based approach can accurately identify the spatial distribution of shading coverage on the photovoltaic module, which is subsequently quantified and used as an input variable for electrical and energy performance analysis.
The electrical power output of the PV module was calculated as:

$$P = V\ \times I \quad (3)$$

To evaluate shading-induced energy degradation, relative energy loss was defined as:

$$Energy\ Loss\ (\%) = \frac{P_0 - P_s}{P_0}\ x\ 100 \quad (4)$$

where P_0 is the output power under minimum shading and P_s is the output power under a specific shading condition.

C. Statistical Analysis

Statistical analysis was conducted sequentially to ensure rigorous evaluation of shading effects.

Pearson Correlation Analysis

Pearson correlation was used to measure the strength and direction of the linear relationship between shading area and PV energy output:

$$r = \frac{\Sigma\,(x_i - \bar{x})\ (y_i - \bar{y})}{\sqrt{\Sigma\,(x_i - \bar{x})^2\ \Sigma\,(y_i - \bar{y})^2}} \quad (5)$$

where:
x_i represents the shading area values,
y_i represents the output current or power values,

$\bar{x}$ and $\bar{y}$ denote the mean values of each variable, respectively.

The value of r ranges from −1 to +1. A value approaching 1 indicates a very strong negative relationship, whereas a value approaching 0 indicates the absence of a linear relationship between the variables.
Interpretation Criteria:

$|r| > 0.7$: strong correlation
$0.4 < |r| \leq 0.70$: moderate correlation
$|r| \leq 0.4$: weak correlation

Linear Regression Analysis

Linear regression was applied to model the quantitative effect of shading area on output current:

$$I = \beta_0 + \beta_1 A_s \tag{6}$$

where:
I represents the output current of the PV module,
A_s represents the percentage of shading area,
β_0 is the intercept (the current when shading approaches zero),
β_1 is the regression coefficient, indicating the rate of current reduction due to increasing shading.

Significance Testing

The significance of regression coefficients was tested using a t-test:

$$t = \frac{\beta_i}{SE(\beta_i)} \tag{7}$$

where:
β_i represents the regression coefficient,
SE (β_i) represents the standard error of the coefficient.
A p-value smaller than the significance level (α=0.05) indicates that the regression coefficient is statistically significant.

Coefficient of Determination

$$R^2 = 1 - \frac{\sum(y_i - \hat{y}_i)^2}{\sum(y_i - \bar{y})^2} \tag{8}$$

The value of R^2 represents the proportion of variance in the photovoltaic (PV) output that can be explained by the object area. A higher R^2 value indicates that the independent variable (object area) provides a better explanation of the variability in the dependent variable (PV output).

One-way Analysis of Variance (ANOVA)

One-way ANOVA was employed to test whether different shading levels result in statistically significant differences in PV energy output:

$$F = \frac{S\,S_B/(k-1)}{S\,S_W/(N-k)} \tag{9}$$

where:
F: ANOVA F-statistic
$S\,S_B$ represents the sum of squares between groups,
$S\,S_W$ represents the sum of squares within groups,
k is the number of shading groups,
N is the total number of observations.
If the p-value obtained from the F-test is less than 0.05, it can be concluded that there are statistically significant differences in energy performance among the shading levels.

Statistical Analysis Workflow

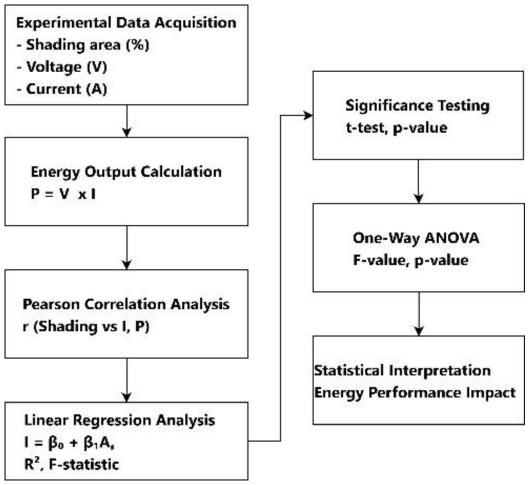

Figure 4 Statistical analysis workflow

Figure 4 presents the statistical analysis workflow, illustrating the sequential process from experimental data acquisition, power calculation, correlation analysis, regression modeling, significance testing, and ANOVA.

III. Results and Discussion

A. Electrical Output under Shading Conditions

Table 1. Electrical Output of PV Module under Various Shading Levels

SHADING (%)	VOLTAGE (V)	CURRENT (A)	POWER (W)
10	12.44	1.94	24.12
30	12.36	1.40	17.30
50	12.23	1.23	15.04
70	12.18	0.85	10.35
100	12.10	0.22	2.66

As shown in Table 1, the electrical output of the photovoltaic (PV) module decreases with increasing shading levels, particularly in terms of current and power output, while voltage remains relatively stable. This behavior occurs because the current generated by a series-connected PV module is limited by the cell receiving the lowest solar irradiance. Under partial shading conditions, the shaded cells reduce the current flowing through the entire module, resulting in a corresponding decrease in output power. In contrast, the module voltage is less sensitive to partial shading and therefore exhibits only relatively small variations within the investigated shading range.

B. Correlation and Regression Results

Pearson correlation analysis shows a very strong negative relationship between shading area and energy-related parameters ($r = -0.98$, $p < 0.001$). These results indicate a very strong and statistically significant negative relationship between shading area and PV energy output.

The estimated regression model is:

$$I = 2.018 - 0.017\, A_S \tag{10}$$

The regression model indicates that each 1% increase in the detected object area results in a decrease in the output current by approximately 0.017 A.
The coefficient of determination (R2=0.961) indicates that 96.1% of the variation in the output current can be explained by the variation in shading area, while the remaining proportion is influenced by other factors such as irradiance fluctuations and environmental conditions.
The model significance test yields:

F-statistic = 198.4
Prob(F-statistic) = 6.27×10^{-7}

These values confirm that the regression model is highly statistically significant. Furthermore, the residual normality test (Jarque–Bera, p=0.913) indicates that the residuals are normally distributed, thereby satisfying the fundamental assumptions of linear regression.

C. ANOVA Results

To ensure that variations in the detected object area produce statistically significant differences in current, voltage, and output power of the PV module, a One-Way Analysis of Variance (One-Way ANOVA) is employed. One-way ANOVA was applied to test differences in energy output across shading levels.

Table 2. One-Way ANOVA Results

Parameter	F-value	p-value
Current	18.62	0.00158
Power	18.83	0.00153

The ANOVA results presented in Table 2 reinforce the correlation and regression analyses conducted previously. Current and power exhibit statistically significant differences across the investigated shading conditions ($p < 0.05$), indicating that the observed reductions in electrical output are associated with increasing shading area rather than random experimental variation. In contrast, the voltage response shows relatively small variation compared with current and power (if the voltage ANOVA is non-significant, $p > 0.05$), reflecting the well-established behavior of series-connected photovoltaic modules in which partial shading primarily limits current while voltage is comparatively less affected. These findings are consistent with the mismatch theory in series-connected PV cells, where the system current is constrained by the cell receiving the lowest irradiance. Accordingly, the proposed computer vision–based shading quantification method provides a practical means of relating image-derived shading coverage to the corresponding changes in photovoltaic electrical performance under the investigated experimental conditions, rather than serving solely as a visual monitoring tool.

D. Shading Area versus Energy Loss

Table 3 summarizes the variation in output power and the corresponding percentage of energy loss under different shading conditions in the photovoltaic (PV) module.

Table 3. Shading Area and Energy Loss

Shading (%)	Power (W)	Energy Loss (%)
10	24.12	0.0
30	17.30	28.3
50	15.04	37.7
70	10.35	57.1
100	2.66	89.0

As shown in Table 3, increasing shading levels result in a substantial reduction in output power, accompanied by a significant increase in energy loss in the photovoltaic (PV) module.

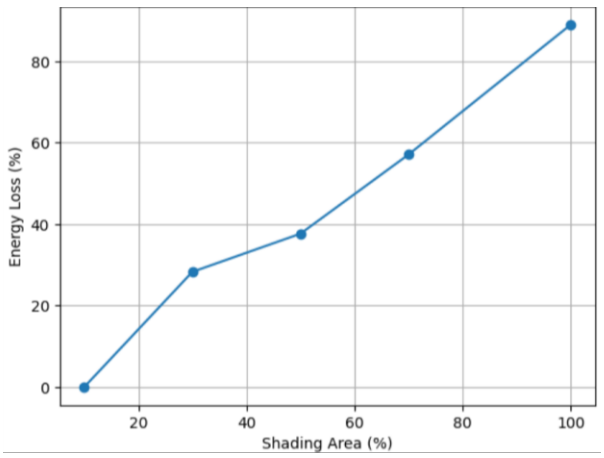

Figure 5 Relationship between shading area and energy loss

Figure 5 shows that output power loss increases as the shading area increases. The linear regression model presented in Equation (10) captures this overall trend with a high coefficient of determination, indicating that the image-derived shading area is a reliable predictor of output power degradation within the investigated experimental range. Although the relationship between partial shading and photovoltaic performance is known to exhibit nonlinear behavior under certain operating conditions, the experimental data obtained in this study are adequately represented by a linear model over the tested shading levels.

E. Discussion

The statistical analysis results consistently show that the image-derived shading area is strongly associated with the electrical performance of the photovoltaic (PV) module under the investigated experimental conditions. The very strong negative Pearson correlation coefficient ($r = -0.98$) indicates that current and output power decrease consistently as the shading area increases. This relationship is consistent with the well-established electrical behaviour of series-connected PV cells under partial shading rather than representing a new physical phenomenon.

As illustrated in Figure 5, the increase in output power loss is not proportional to the increase in shading area. At relatively low shading levels, the reduction in output power is moderate; however, as the shaded area becomes larger, the power loss increases more rapidly. This behaviour is attributed to the electrical mismatch effect in series-connected photovoltaic cells, where the current of the entire module is constrained by the cell receiving the lowest solar irradiance. Consequently, additional shaded cells reduce the operating current of the module disproportionately, leading to a greater decline in output power than would be expected from the increase in shaded area alone. Under more severe shading conditions, the activation of bypass diodes and changes in the operating point of the module may further contribute to the observed nonlinear trend.

The linear regression model yielded a coefficient of determination of $R^2 = 0.961$, indicating that the image-derived shading area explains a substantial proportion of the variation in the measured PV output within the investigated experimental range. However, given the limited number of experimental observations ($n = 5$), this result should be regarded as preliminary evidence rather than a definitive predictive model. Instead, the regression analysis demonstrates the feasibility of the proposed computer vision–based shading quantification method for relating spatial shading measurements to output power degradation under controlled laboratory conditions. Although the overall experimental trend can be adequately represented by a linear regression within the investigated shading range, Figure 5 suggests that the underlying physical behaviour is more complex and may become increasingly nonlinear under broader shading conditions. Future studies with a larger number of shading levels are therefore needed to investigate this behaviour in greater detail.

The ANOVA results further confirm that different shading levels produce statistically significant variations in photovoltaic electrical performance, indicating that the observed changes in current and output power are attributable to increasing shading coverage rather than random experimental variation. These findings are consistent with the mismatch effect in series-connected photovoltaic cells, where the current of the entire module is constrained by the cell receiving the lowest solar irradiance.

Overall, the contribution of this study lies not in establishing a new relationship between shading and photovoltaic performance, which has been extensively reported in previous studies, but in demonstrating that computer vision can provide a practical, non-contact, and quantitative means of measuring physical shading coverage and relating it to photovoltaic output power degradation. This approach addresses the limitation of previous studies that relied primarily on geometric simulations or irradiance-based analyses without directly quantifying physical shading on the PV surface.

IV. Conclusion

Based on the results of this study, the following conclusions can be drawn:

1. The proposed computer vision–based statistical framework successfully transforms visual shading information into a quantitative indicator for evaluating the impact of partial shading on photovoltaic (PV) energy performance.
2. The correlation analysis demonstrates a strong relationship between shading conditions and energy degradation, indicating that shading features extracted from images can effectively represent PV performance losses.
3. The linear regression model provides reliable predictive capability, while the analysis of variance (ANOVA) confirms the statistical significance of the proposed approach. These results demonstrate the robustness and validity of the framework for analysing partial shading effects in static PV systems.
4. The proposed method offers a practical and cost-effective alternative for assessing shading-induced energy losses, supporting improved monitoring and performance evaluation of photovoltaic installations.
5. Future research should validate the proposed framework using real-world outdoor photovoltaic installations under varying weather and operational conditions.
6. Additional environmental parameters, such as solar irradiance, temperature, humidity, and seasonal variations, should be incorporated to improve the accuracy and reliability of energy yield prediction.
7. Further studies may explore the integration of machine learning and real-time monitoring systems to enhance predictive performance and support intelligent photovoltaic energy management.

V. References

[1] T. Stalcup *et al.*, "On-grid performance of REhnu's 8-mirror CPV-T tracker," *AIP Conference Proceedings*, vol. 1881, no. September, 2017, doi: 10.1063/1.5001411.

[2] M. Gupta, A. Arya, U. Varshney, J. Mittal, and A. Tomar, "Progress in Engineering Science A review of PV power forecasting using machine learning techniques," *Progress in Engineering Science*, vol. 2, no. 1, p. 100058, 2025, doi: 10.1016/j.pes.2025.100058.

[3] C. Gutiérrez, M. Á. Gaertner, O. Perpiñán, C. Gallardo, and E. Sánchez, "A multi-step scheme for spatial analysis of solar and photovoltaic production variability and complementarity," *Solar Energy*, vol. 158, no. September 2017, pp. 100–116, 2017, doi: 10.1016/j.solener.2017.09.037.

[4] D. W. Jiaxuan Jing, Yong Zhou, Lingyu Wang, Yanfeng Liu, "The spatial distribution of China's solar energy resources and the optimum tilt angle and power generation potential of PV systems," *Energy Conversion and Management*, vol. 283, 2023, doi: https://doi.org/10.1016/j.enconman.2023.116912.

[5] A. Makkulau, S. Samsurizal, and S. Kevin, "Karakteristik Temperatur Pada Permukaan Sel Surya Polycrystalline Terhadap Efektifitas Daya Keluaran Pembangkit Listrik Tenaga Surya," *Jurnal Ilmiah Sutet*, vol. 10, no. 2, pp. 69–78, 2020, doi: 10.33322/sutet.v10i2.1291.

[6] A. Makkulau and Christiono; Samsurizal, "Characteristics of Temperature Changes Measurement on Photovoltaic Surfaces Against Quality of Output Current on Solar Power Plants," in *2019 International Conference on Technologies and Policies in Electric Power and Energy, TPEPE 2019*, 2019, pp. 20–23. doi: 10.1109/IEEECONF48524.2019.9102630.

[7] A. Makkulau, A. Suyuti, A. A. Ilham, and S. M. Said, "Assessment and Optimization of Rooftop Photovoltaic Potential: A Case Study of Subsidized Type-36 Residential Buildings in Indonesia," IEEE, 2025, pp. 603–608. doi: 10.1109/ICATEI67676.2025.11405068.

[8] A. B. Acharya, L. E. Norum, and D. Sera, "A Shadow Tolerant Configuration for PV Integration to Grid using Modular Multilevel Converter," *Proceedings of 2018 IEEE International Conference on Power Electronics, Drives and Energy Systems, PEDES 2018*, pp. 1–6, 2018, doi: 10.1109/PEDES.2018.8707829.

[9] G. Sreenivasa Reddy, T. Bramhananda Reddy, and M. Vijaya Kumar, "Shadow dispersion of PV Array under variable irradiance for superior power Generation by Magic Square Configuration," *International Journal of Engineering & Technology*, vol. 7, no. 1.8, p. 172, 2018, doi: 10.14419/ijet.v7i1.8.11543.

[10] A. Makkulau, M. Fikri, Samsurizal, and Christiono, "The effect of temperature changes on photovoltaic surface against the output current of polycristaline solar power plant," *AIP Conference Proceedings*, vol. 2680, no. 1, p. 20151, Dec. 2023, doi: 10.1063/5.0128466.

[11] A. Mansur, "Analisa Dampak Bayangan Modul Terhadap Output PLTS," *Energi & Kelistrikan*, vol. 11, no. 2, pp. 160–169, 2019, doi: 10.33322/energi.v11i2.746.

[12] Z. Yun and Y. Chen, "Research on the Output Characteristics of Series PV Array with Partial Shadow," *Proceedings of 2018 2nd IEEE Advanced Information Management, Communicates, Electronic and Automation Control Conference, IMCEC 2018*, no. Imcec, pp. 2443–2449, 2018, doi: 10.1109/IMCEC.2018.8469346.

[13] S. D. P. Samsurizal, M. Fikri, and Christiono, "Dampak Bayangan Pada Panel Surya Terhadap Daya Keluaran Photovoltaic," *Setrum : Sistem Kendali-Tenaga-elektronika-telekomunikasi-komputer*, vol. 9, no. 2, pp. 50–62, 2020, doi: 10.36055/setrum.v9i2.9202.

[14] A. Makkulau, Andi; Pasra, Nurmiati; Kumala Sultan BP, "Pendeteksi Objek Pada Permukaan Modul Surya Menggunakan Simulasi Perangkat Lunak," F. Mayasari, Ed., Makassar: Universitas Hasanuddin, 2022, pp. 93–96.

[15] A. Mansur, "Analisa Kinerja Plts on Grid 50 Kwp Akibat Efek Bayangan Menggunakan Software Pvsyst," *Transmisi*, vol. 23, no. 1, pp. 28–33, 2021, doi: 10.14710/transmisi.23.1.28-33.

[16] T. Paphapote, W. Bamrungsawat, and T. Wongwuttanasatian, "Inclination and Inter-Row Spacing Optimization for 12 MW Floating Photovoltaic System with Shading Loss and Financial Analysis," Results in Engineering, vol. 27, Art. no. 106362, 2025, doi: 10.1016/j.rineng.2025.106362.

[17] T. Ma, H. Yang, and L. Lu, "Development of a Model to Simulate the Performance Characteristics of Crystalline Silicon Photovoltaic Modules/Strings/Arrays," Solar Energy, vol. 100, pp. 31–41, 2014, doi: 10.1016/j.solener.2013.11.018.

[18] M. Baqir and H. K. Channi, "Analysis and Design of Solar PV System Using PVsyst Software," Materials Today: Proceedings, vol. 48, pp. 1332–1338, 2022, doi: 10.1016/j.matpr.2021.09.029.

[19] M. Parhamfar and A. Zabihi, "Comprehensive Design of a 100-kilowatt Solar Power Plant with Bifacial Technology in PVsyst for Arak, Iran," Solar Energy Advances, vol. 5, Art. no. 100092, 2025.

[20] Y. Lu, L. Wang, J. Wang, P. Liu, R. Rafee, S. Rashidi, and G. Li, "Effect of Partial Shading on the Performance of Concentrated Photovoltaics: A Simulation and Experimental Study Based on the Double-Diode Model," Energy, vol. 348, Art. no. 140571, 2026, doi: 10.1016/j.energy.2026.140571.

[21] M. Khan, M. Ferdous, and S. Chowdhury, "Sustainable Development of Solar Power Through the Investigation of Partial Shading Effect of Solar Module in Terms of Experimental Setup and MATLAB Simulation," Procedia Computer Science, vol. 252, pp. 702–707, 2025, doi: 10.1016/j.procs.2025.01.078.

[22] S. Sarkar, K. U. Rao, V. Prema, M. S. Bhaskar, S. Padmanaban, and J. Bhargav, “A Model for Effect of Partial Shading on PV Panels with Experimental Validation,” Energy Reports, vol. 12, pp. 3460–3469, 2024, doi: 10.1016/j.egyr.2024.09.015.
[23] N. Kalyani, P. Winston, P. Murugesan, and S. Devakirubakaran, “Single Input Multi Output Converter Based Partial Shading Mitigation in Solar Photovoltaic Systems,” Solar Energy, vol. 308, Art. no. 113135, 2026.
[24] S. Gall, M. F. Al Rayes, F. Hermerschmidt, E. Nandayapa, and E. J. W. List-Kratochvil, “On the Influence of Partial Shading and the Use of Bypass Diodes on Perovskite-Based Single-Junction Photovoltaic Mini-Modules,” Solar Energy Materials and Solar Cells, vol. 297, Art. no. 114130, 2026, doi: 10.1016/j.solmat.2025.114130.
[25] A. Makkulau, M. Fikri, Samsurizal, and Christiono, “Analysis of the Effect of Shading Modification on the Electrical Power Characteristics of Solar Panels Using Linear Regression,” in Proceedings of the Seminar Nasional Energi, Ketenagalistrikan, dan Teknik Elektro Indonesia (SNEKTI), 2023.
[26] I. Shamta, F. Demir, and B. Erdem, “Predictive Fault Detection and Resolution Using YOLOv8 Segmentation Model: A Comprehensive Study on Hotspot Faults and Generalization Challenges in Computer Vision,” Energy Reports, vol. 15, 2024.
[27] L. Chen, S. Fan, S. Sun, S. Cao, T. Sun, P. Liu, H. Gao, Y. Zhang, and W. Ding, “A Detection Model for Dust Deposition on Photovoltaic (PV) Panels Based on Light Transmittance Estimation,” Energy, vol. 322, Art. no. 135284, 2025, doi: 10.1016/j.energy.2025.135284.
[28] E. G. Vourkos, R. A. Agathokleous, A. S. Panayides, S. A. Kalogirou, and E. G. Christoforou, “Improving Photovoltaics Hotspot and Dirt Accumulation Detection with Computer Vision: A Systematic YOLO Model Comparison Based on Field Aerial Images,” Solar Energy, vol. 288, Art. no. 113046, 2025.
[29] W. Ji, M. Wang, H. Fang, K. Wu, X. Wang, and B. Xu, “Review of Key Technologies and Development Trends of Photovoltaic Panel Cleaning,” Renewable and Sustainable Energy Reviews, vol. 411, Art. no. 115281, 2026.
[30] M. de Jesus dos Santos Rodrigues, J. de Arimatéia Alves Vieira Filho, D. C. Estumano, I. Ruy de Parijós Junior, M. A. Barros Galhardo, C. A. Beltran Castañón, and W. N. Macêdo, “Cost-Effective and Portable Device for Partial Shading Assessment in Photovoltaic Modules Using RGB Imaging,” Energy, vol. 344, Art. no. 139948, 2026, doi: 10.1016/j.energy.2026.139948.
[31] R. Cavieres, R. Barraza, D. Estay, and P. Valdivia-Lefort, “Automatic Soiling and Partial Shading Assessment on PV Modules Through RGB Images Analysis,” Solar Energy, vol. 226, pp. 857–868, 2022, doi: 10.1016/j.solener.2021.08.084.
[32] B. Liu, X. Wang, K. Sun, Q. Bi, Y. Li, and X. Yang, “A Novel Data-Driven State Evaluation Approach for Photovoltaic Arrays in Uncertain Shading Scenarios,” Energy, vol. 312, Art. no. 133533, 2024, doi: 10.1016/j.energy.2024.133533.
[33] N. Kellil, A. Mellit, C. Rus-Casas, and M. Benghanem, “Hybrid Vision Transformer Model for Defect Classification in Photovoltaic Modules Using Thermographic Imaging: Leveraging Self-Attention Mechanisms for Enhanced Accuracy,” Renewable Energy, vol. 256, Art. no. 124138, 2026, doi: 10.1016/j.renene.2025.124138.